Subdiffusive dynamics and hydrodynamic fluctuations: how the latter affect the former.

Subdiffusive dynamics and hydrodynamic fluctuations: how the latter affect the former.

Evangelos Bakalis* **and Francesco Zerbetto**
Dipartimento di Chimica "G. Ciamician", Universita di Bologna, Bologna, Italy
E-mail: evangelos.bakalis2@unibo.it

Abstract. The characteristics of subdiffusion are influenced by hydrodynamic fluctuations, not the scaling of the mean square displacement (MSD) at the long time limit, but rather the transition of this property from ballistic behaviour at early times to its final scaling at large times. Additionally, since a significant portion of the normalised velocity autocorrelation function (NVAF), a widely used motion descriptor, no longer adequately describes the anti-persistent character that is typical of a subdiffusive motion, it is also impacted by these fluctuations. The combined findings can lead to misleading conclusions if hydrodynamic fluctuations are not taken into account. Diffusing and vorticity time scales are crucial for the way the motion turns into the final subdiffusion dynamics, whose exponent is determined by the scaling of the friction.

1. Introduction

Anomalous diffusion plays a key role in many phenomena across different branches of science. [1] The Langevin equation is a simple phenomenological description of the balance of the forces exerted on a target "particle", and it contains the first and second-order time derivatives of the particle position. Assuming the existence of non-integer time derivatives acting on the position of the target particle, we write the fractional generalised Langevin equation. [2]

$$m_c D_t^{\mu} x(t) + \int_0^t \gamma(t-t')_c D_t^{\nu} x(t') dt' + F_{BB}(t) + F_{con}(t) + F_{per}(t) = \xi(t) \tag{1}$$

where ${}_cD_t^{\mu}$ denotes the fractional derivative defined by

$${}_cD_t^{\mu} x(t) = \frac{1}{\Gamma(n-\mu)} \left(\frac{d}{dt}\right)^n \int_c^t \frac{x(t)}{(t-u)^{\mu-n+1}} dt, n-1 \leq \mu < n, t > c \tag{2}$$

where $\Gamma()$ is the gamma function and the index c denotes the lower limit of the integral. Eq.(2) returns the Weyl fractional integral for $c \to -\infty$, and the Riemann-Liouville fractional derivative for $c = 0$. [3]. We set $c = 0$ and for shake of simplicity we write D_t^{μ} instead of ${}_0D_t^{\mu}$. It is hold true that $1 < \mu \leq 2$, and $0 < \nu \leq 1$; for $\mu = 2$ and $\nu = 1$, eq.(1) returns the generalized Langevin equation. The term $\gamma(t)$ expresses the memory effects introduced by the friction term, $F_{con}(t)$ is any conservative force usually taken as a harmonic restoring force, $F_{con}(t) = kx(t)$, k being the stiffness, $F_{per}(t)$ is any periodic force acting on the target particle, and $\xi(t)$ is the overall random force that can result from both additive and/or multiplicative random forces of different origins. Typically, the total random force is thought of as having

a zero mean and a variance to be estimated. $F_{BB}(t) = \frac{m_f}{2}\dot{u}(t) + \gamma_0\sqrt{\frac{\tau_v}{\pi}}{}_{-\infty}D_t^{\frac{1}{2}}\dot{u}(t)$ is the Boussinesq–Basset (BB) force and describes hydrodynamic fluctuations (HFs). [4, 5] The BB force incorporates two terms. The first term stands for the acceleration of the liquid molecules displaced by the tracer particle; m_f is the mass of the fluid element with a volume equal to that of the particle. The second term, written as a fractional semi-derivative, expresses the convolution of a time dependent friction coefficient with the acceleration and is weighted by the square root of the vorticity time, τ_v. Notice that $\gamma_0 = 6\pi\eta r$ is the bare friction coefficient, with η being the dynamic viscosity of the medium, and r the radius of the target particle. The lower limit of the convolution integral in BB force t_0 can be set to $-\infty$, and thus the contribution $\gamma_0\sqrt{\frac{\tau_v}{\pi}}{}_{-\infty}D_0^{\frac{1}{2}}\dot{u}(t) = \gamma_0\sqrt{\frac{\tau_v}{\pi}}\int_{-\infty}^{0}(t-t')^{-\frac{1}{2}}\frac{du(t')}{dt'}dt'$ corresponds to a colored noise caused by BB force, whose correlation goes as $< \xi_{BB}(t)\xi_{BB}(0) > \sim t^{-\frac{3}{2}}$. [6, 7] We cite some recent literature that provides more details on the impact of HFs on the diffusive motion of a particle. [8, 9, 10, 11, 12, 13]

2. Single Particle Tracking and Mathematical Modelling

Single Particle Tracking (SPT) is a class of non-invasive techniques capable of tracing the spatial position of single molecules or other nanoscopic entities as a function of time. These techniques have proven to be particularly useful for observing the spatiotemporal dynamics of biological processes both in vitro and in vivo due to their high resolution and real-time observational capabilities. [14] On the basis of equation (1), a force term that expresses the interaction of the applied machinery with the observed particle can be added to model the motion captured by SPT techniques. [15, 16] Experiments conducted under low to moderate doses of light irradiation, which can be safely considered to not apply any additional force to the observed nanoentities, are of particular interest. [17] Such a system can be described by eq.(1) with $\mu = 2$, $\nu = 1$, $F_{con} = 0$, and $F_{per} = 0$

$$(m + \frac{m_f}{2})\frac{d^2x(t)}{dt^2} + \int_0^t \gamma(t-t')\frac{dx(t')}{dt'}dt' + \gamma_0\sqrt{\frac{\tau_v}{\pi}}\int_0^t (t-t')^{-\frac{1}{2}}\frac{du(t')}{dt'}dt' = \xi(t) \tag{3}$$

In equation (3), the memory kernel appears in the generalised Stokes force, it has meaning in distributional sense, and it is equal to zero for $t < 0$. For constant drag coefficient, the memory kernel is expressed through the Dirac delta function, $\gamma(t-t') = 2\gamma_0\delta(t-t')$. When HFs are present, a constant friction force cannot be used because of a non-stable flow. In this work, we consider that the friction force is expressed as a one-parameter Mittag-Leffler (ML) function, $\gamma(t) = \frac{\gamma_0}{\tau_f^\alpha}E_\alpha(-(t/\tau_f)^\alpha)$, where $0 < \alpha < 1$ is the scaling exponent that determines the dynamics of the target particle in the long time limit due to the fluctuation dissipation relation. [18, 19, 13] τ_f is the characteristic memory of the friction, and $E_a(z) = \sum_{n=0}^{\infty}\frac{z^a}{\Gamma(an+1)}$ is the one-parameter ML function. [20, 21] Our choice assures that friction goes to zero for $t \to 0$ and it behaves as power law for large times. [22] A more general equation than eq.(3) recently received its general solution. [13] Only the mathematical expressions required for the discussion section are given in this article; the full mathematical derivation is covered elsewhere. [13]

The generalized response function in Laplace domain reads [13]

$$R(s) = \frac{s^{\delta-2} + \tau_f^{-\alpha}s^{\delta-\alpha-2}}{1 + \frac{\sqrt{\tau_v}}{\tau_d}s^{-\frac{1}{2}} + \tau_f^{-\alpha}s^{-\alpha} + \frac{\sqrt{\tau_v}}{\tau_d\tau_f^\alpha}s^{-\alpha-\frac{1}{2}} + \frac{1}{\tau_d\tau_f^\alpha}s^{-2}} \tag{4}$$

Three time scales are present in equation (4), that is, the diffusion time, $\tau_d = \frac{m_{tot}}{\gamma_0}$ with $m_{tot} = m + \frac{m_f}{2}$, the vorticity time $\tau_v = \frac{r^2\rho_f}{\eta}$ that provides the loss of the hydrodynamic memory, and the memory of the friction τ_f, notice that ρ_f is the density of the medium. Their competition

reveals interesting dynamics, see below. The exponent δ is an auxiliary variable, it takes the values of $1, 0, -1$. For $\delta = -1$, the inversion of equation (4) in the time domain returns the mean square displacement (MSD)

$$\frac{\Delta x^2(\tau)}{2k_BT/m_{tot}} = R(|\tau|)|_{\delta=-1} \tag{5}$$

where k_BT is the Boltzmann's constant times the temperature of the bath. For $\delta = 1$, the inversion of equation (4) in the time domain returns the normalized velocity autocorrelation function (NVAF).

$$\frac{C_u(\tau)}{C_u(0)} = \frac{m}{m_{tot}} R(|\tau|)|_{\delta=-1} \tag{6}$$

Considering the absence of HFs, $\tau_v = 0$, equation (4) in the time domain reads

$$R(\tau) = \tau^{1-\delta}\{\frac{1}{\Gamma(2-\delta)} - \frac{1}{\tau_d}\tau^{2-\alpha}E_{2-\alpha,4-\delta-\alpha}(-\frac{1}{\tau_d}\tau^{2-\alpha})\}, \tau > \tau_f \tag{7}$$

where $E_{a,b}(z)$ is a two-parameter ML function. [3] Equation (7) will be compared to the general solution when HFs are present in order to underline the impact of the latter on the subdiffusive motion of the tracer particle.

3. Results and Discussion

The inversion of Eq.(4) in the time domain is made through the multinomial ML function, and its behavior for short and large times as well as its behavior for much broader time windows is explicitly given. [13] In this work, we estimate the MSD and the NVAF by using the numerical inversion of Eq. (4), [23, 24] and we examine the competition of diffusing and vorticity time. Of note is that these two time scales do not take random values independent of each other but fulfil the following condition: $\frac{\tau_d}{\tau_v} = \frac{2}{9}\frac{m_p}{m_f} + \frac{1}{9}$[1]. According to this condition, the minimum value of the diffusing time can be one nineth of the vorticity time when the mass of the fluid molecules is much larger than the mass of the target particle. We consider the cases; i) $\frac{\tau_d}{\tau_v} = 10^2$, which means that $\frac{m_p}{m_f} = 449.5$ and we choose the values $\tau_d = 10^{-4}$ sec, $\tau_v = 10^{-6}$ sec, and $\tau_f = 10^{-7}$ sec. ii) $\frac{\tau_d}{\tau_v} = 0.1116$, which means that $\frac{m_p}{m_f} = \frac{1}{449.5}$ and we choose the values $\tau_d = 1.116 \times 10^{-5}$ sec, $\tau_v = 10^{-4}$ sec, and $\tau_f = 10^{-7}$ sec. iii) $\frac{\tau_d}{\tau_v} = 0.3333$, which means that $\frac{m_p}{m_f} = 1$ and we choose the values $\tau_d = 3.333 \times 10^{-5}$ sec, $\tau_v = 10^{-4}$ sec, and $\tau_f = 10^{-7}$ sec.

The behavior of NVAF and MSD in the absence of HFs is only discussed in Figure 1 for two limit values of the scaling exponent α, namely, 0.05 and 0.9, given that the behavior of the rest values of α lies between these two. When it is feasible, they are shown in the remaining figures to visually illustrate the effects that the presence of hydrodynamic fluctuations introduces to the random motion. The NVAF for $\alpha = 0.05$, (Figure 1a, orange line) retains a strong persistent behaviour for time moments greater than the diffusing time, and then it starts exhibiting intense fluctuations around zero, denoting that the environment itself acts as a restoring force when the scaling exponent is close to zero. [11] The vertical line at $t = 1.4 \times 10^{-2}$ indicates the first crossing zero of the NVAF and marks the end of the initial sub-ballistic motion, see the MSD orange line in Figure 1b, and the transition to the final subdiffusive motion driven by the scaling of the friction term. Notice that the MSD reaches a kind of plateau, it actually has a slope equal to the value of $\alpha = 0.05$, assuring again the role of the environment as a restoring force. For $\alpha = 0.9$, the NVAF is always positive (persistent motion), Figure 1a dark red line, with the

[1] By using the definitions, $\tau_d = \frac{m_{tot}}{\gamma_0}$, $\tau_v = r^2\frac{\rho_f}{\eta}$, $\gamma_0 = 6\pi\eta r$, one can easily arrive to it.

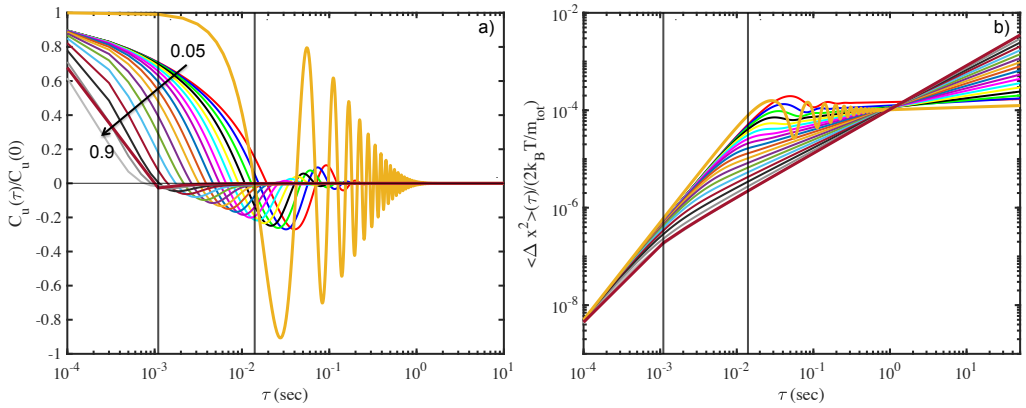

Figure 1: It displays the NVAF (Figure 1a) and the MSD (Figure 1b) for the first system, that is, $\tau_d = 10^{-4}$ sec, $\tau_v = 10^{-6}$ sec, and $\tau_f = 10^{-7}$ sec, $m_p >> m_f$. The arrow in Figure 1a indicates how the exponent α increases from 0.05 to 0.9 with a step of 0.05. The colour code in Figure 1a and 1b describes the same α. In addition, in each panel, the NVAF and the MSD in the absence of HFs for two extreme cases, $\alpha = 0.05$ orange line and $\alpha = 0.9$ dark red line, are shown where we made use of eqs.(5-7). The two vertical lines at each panel, $t = 1.1 \times 10^{-3}$ and $t = 1.4 \times 10^{-2}$ stand for the first zero crossing of the NVAF and also indicate the passage from the initial transient sub-ballistic motion to subdiffusion governed by the scaling exponent α: the first vertical line for $\alpha = 0.9$ and the second for $\alpha = 0.05$, eqs (5-7).

exception of a very small peak below zero at $t = 1.1 \times 10^{-3}$ sec, where also a vertical line has been drawn, after which the motion turns uncorrelated. In Figure 1b, for the same exponent and colour, the motion is superdiffusive up to the turning point $t = 1.1 \times 10^{-3}$ sec, and then it turns subdiffusive with a scaling exponent equal to 0.9. It is significant to note that depending on the scaling of the friction term, the initial motion can range from sub-ballistic to super-diffusion; the larger the friction scaling, the smaller the exponent for the MSD, but always in the super-diffusion regime. HFs change this behaviour in many senses, even when $m_p >> m_f$ that is depicted in Figure 1. The orange and red lines in Figure 1a represent the NVAF in the absence and presence of HFs, respectively, for $\alpha = 0.05$. In the presence of HFs (red line), the NVAF loses its strong, persistent nature, as shown in their absence (orange line). Aside from that, HFs also smooth the environmental restoring role out (see the differences between the orange and red lines), and they increase the formed memory (first crossing zero). The strong fluctuations around zero for non-present HFs are replaced by smooth fluctuations, and the maximum of them is reduced as the value of α increases (black arrow). The MSD, in the presence of HFs, supports the smoothing of the strong fluctuations for small α. It also underlines the turning point of the initial superdiffusive motion to the final subdiffusive motion governed by the scaling exponent α, which is not affected by the presence or absence of HFs. The turning point depends on the value of α, see the two vertical lines in the right panel of Figure 1, where the first at $t = 1.1 \times 10^{-3}$ underlines the turning point for $\alpha = 0.9$ and the second at $t = 1.4 \times 10^{-2}$ the turning point for $\alpha = 0.05$. By using as mark the first vertical line we estimate the scaling of the MSD for this short regime. The results are displayed in Figure 4a, where it is clear that for $\alpha < 0.6$, the scaling exponent β of the MSD is greater than 1.9 (sub ballistic motion), and for $\alpha = 0.9$, $\beta \sim 1.3$ in this time range.

Figures 2a and 2b show the NACF and MSD, respectively, of the target particle when the vorticity time is greater than the diffusing time, the condition $m_p << m_f$ holds true. The NVAF loses much faster its persistent character with respect to what happens when HFs are not

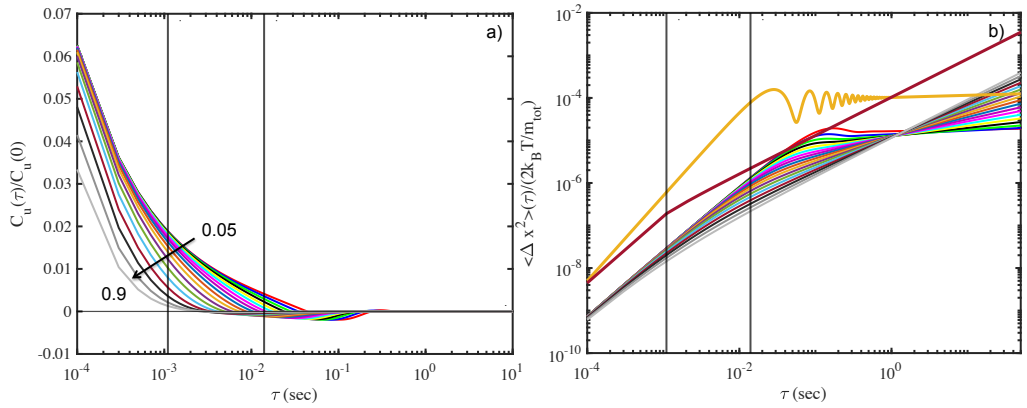

Figure 2: It displays the NVAF (Figure 2a) and the MSD (Figure 2b) for the second case, $m_p << m_f$, $\tau_d = 1.116 \times 10^{-5}$ sec, $\tau_v = 10^{-4}$ sec, and $\tau_f = 10^{-7}$ sec. The arrow in Figure 2a indicates how the exponent α increases from 0.05 to 0.9 with a step of 0.05. The colour code in both of them describes the same α. The vertical lines indicate the crossover in the dynamics in the absence of HFs for the two extreme values of α, see Figure 1 for details.

present (lines not drwan), the oscillating character is lost, the NVAF is positive, and only for small values of α exists a small time window that captures anti-persistent behaviour. In addition, the MSD (Figure 2b) takes smaller values in relation to the absence of HFs underlying thus that the particle, explores a smaller space, takes smaller steps, or has a reduced diffusion coefficient in general. Its initial super diffusive motion turns to the final subdiffusion dictated by the friction term; however, fitting the dynamics for time moments smaller than 1.1×10^{-3} the scaling of the MSD is about 1.5, see Figure 4b, for $\alpha \leq 0.6$ and goes down to 1.2 for $\alpha = 0.9$. The value of 1.5 is the fingerprint of HFs on the scaling exponent β of MSD, [6, 7] which means that for $\alpha \leq 0.6$ HFs dominate the motion in this short time window.

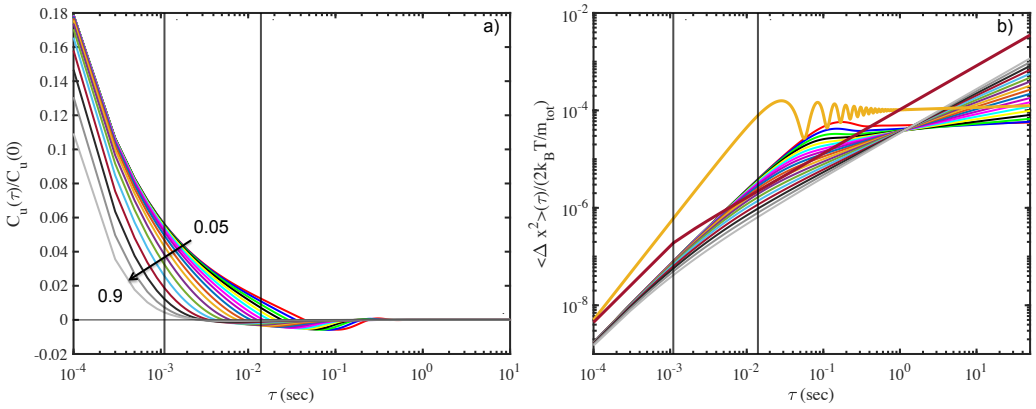

Figure 3: It displays the NVAF (Figure 3a) and the MSD (Figure 3b) for the third case, $m_p = m_f$, $\tau_d = 3.33 \times 10^{-5}$ sec, $\tau_v = 10^{-4}$ sec, and $\tau_f = 10^{-7}$ sec. The colour code in both describes the same α. The vertical lines indicate the crossover in the dynamics in the absence of HFs for the two extreme values of α, see Figure 1 for details.

Figures 3a and 3b illustrate the NVAF and MSD, respectively, of a target particle in the presence of HFs when the mass of the diffusing particle is equal to the mass of the fluid molecules

for the same volume element. The NVAF loses its correlation fast, but the first crossing of zero takes place at time moments larger with respect to the absence of HFs and indicates the formation of a larger memory. Again, we observe a very small time window for low values of the friction scaling exponent, for which the motion shows signs of anti-persistent behaviour. The MSD confirms the findings of NVAF, there are two distinct time regimes. In the first one, for $t < 1.1 \times 10^{-3}$, the target particle undergoes a super diffusion with scaling exponent $1.5 < \beta < 1.6$ and for $0 < \alpha < 0.6$, while for $\alpha > 0.6$ this exponent goes down to 1.3, see Figure 4c. In the second regime, the friction force dominates the motion and imposes its scaling with the particle following subdiffusive motion.

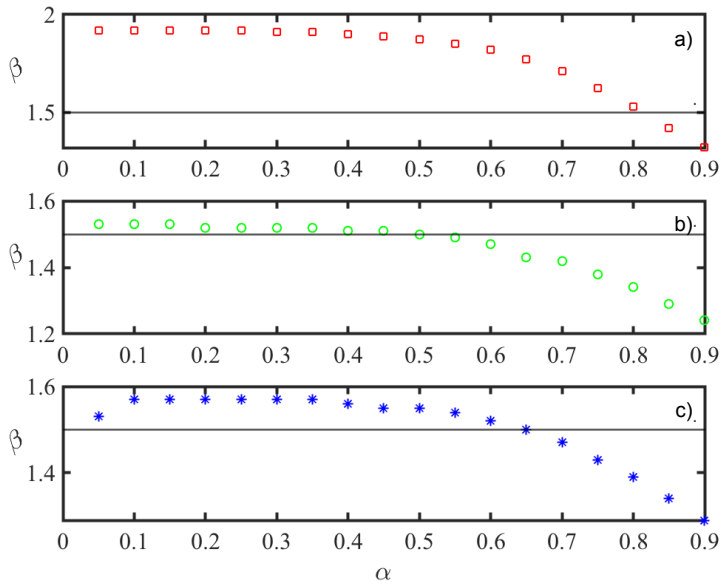

Figure 4: Scaling exponent of MSD (β) versus the scaling exponent of the friction term (α) for $\tau \leq 0.0011$ sec. Figure 4a for the first case, Figure 4b for the second, and Figure 4c for the third.

Figures 4a, 4b, and 4c display the scaling of the exponent β of the MSD as a function of the scaling exponent α of the friction term for early times of the motion where it is still superdiffusive. In the absence of HFs (Figure 4a) the target particle follows a sub-ballistic motion for a broad range of values of α. The presence of HFs change this behaviour, lowering the scaling exponent to 1.5 when HFs dominate the motion (Figure 4b) or to a value a little above 1.5 (Figure 4c) when the mass of the target particle is equal to the mass of the displaced liquid.

4. Conclusion

The presence of HFs leaves fingerprints on the widely used statistical measures used for the understanding of random motions, the NVAF and the MSD. Motion modelled by a one-parameter ML friction term starts ballistically for short times and then makes a smooth transition to the final subdiffusive motion governed by the scaling exponent α of the friction term. In addition, HFs lower the scaling exponent of the MSD in the superdiffusive regime, and when dominant, this scaling is equal to 1.5. Their presence is more evident in the form of NVAF, whose anti-persistent behaviour is washed out, and only very small traces of this behaviour are present in small time windows when the scaling of the friction force is very small. Furthermore, their presence extends the formed memory, and this is the basic mechanism for cancelling the anti-persistent of the dominating subdiffusion on long time scales.

References

[1] Hofling F and Franosch T 2013 *Rep. Prog. Phys.* **76** 046602
[2] dos Santos M A F 2019 *Chaos, Solitons and Fractals* **124** 86 – 96
[3] Podlubny I 1999 *Fractional Differential Equations* (Academic Press) URL `https://www.hbuk.co.uk/ap/`
[4] Boussinesq A B 1885 *C. R. Acad. Sci. III* **100** 935 – 937
[5] Basset A B January 1, 1888 *A Treatise in Hydrodynamics* (University of Michigan Library)
[6] Felderhof U B 1978 *J. Phys. A: Math. Gen.* **11** 921 – 927
[7] Mainardi F, Mura A and Tampieri F 2009 *Mod. Probl. Stat. Phys.* **8** 3 – 23
[8] Tothova J, Vasziiona G, Glod L and Lisy V 2011 *Eur. J. Phys.* **32** 645
[9] Grebenkov D S, Vahabi M, Bertseva E and Forro Laszlo J S 2013 *Phys. Rev. E.* 040701(R)
[10] Grebenkov D S and Vahabi M 2014 *Phys. Rev. E.* 012130
[11] Viñales A D and Paissan G H 2014 *Phys. Rev. E* **90** 062103
[12] Makris N 2021 *Phys. Fluids* **33** 072014
[13] Bakalis E and Zerbetto F 2023 *Physica A* **620** 128780
[14] Manzo C and Garcia-Parajo M 2015 *Rep. Prog. Phys.* **78** 124601
[15] Franosch T, Grimm M, Belushkin M, Mor F M, Foffi G, Forro L and Je S 2011 *Nature* **478** 85 – 88
[16] Kheifets S, Simha A, Melin K, Li T and Raizen M G 2014 *Science* **343** 1493 – 1496
[17] Guernelli M, Bakalis E, Mavridi-Printezi A, Petropoulos V, Cerulo G, Zerbetto F and Montalti M 2022 *Nanoscale* **14** 7233–7241
[18] Kubo R 1966 *Rep. Prog. Phys.* **29** 255 – 284
[19] Fodor Grebenkov D S, Visco P and van Wijland F 2015 *Physica A* **422** 107 – 112
[20] Mittag-Leffler M G 1902 *C. R. Acad. Sci. Paris (Ser. II)* **136** 937 – 939
[21] Mittag-Leffler M G 1904 *Rend. Accad. Lincei* **13** 3 – 5
[22] Mainardi F and Gorenflo R 2000 *J. Comput. Appl. math.* **118** 283 – 299
[23] Garrappa R 2015 *SIAM Journal of Numerical Analysis* **53** 1350 – 1369
[24] McClure T 2023 *Numerical Inverse Laplace Transform, MATLAB Central File Exchange* (MATLAB, The MathWorks Inc.) URL `https://www.mathworks.com/matlabcentral/fileexchange/39035-numerical-inverse-laplace-transform`